



Influence of Mechanical Alloying Time on Microstructure and Wear Behaviors of Fe–Cu–C Alloy

Elvan Büyükkayacı¹ · İjlal Şimşek² · Dursun Özyürek³

Received: 29 November 2019 / Accepted: 19 March 2020 / Published online: 14 April 2020
© The Korean Institute of Metals and Materials 2020

Abstract

In the present study, the influence of mechanical alloying time on microstructure and wear behavior was investigated for Fe–Cu–C alloy produced with powder metallurgy method. Within the scope of the study, Fe, Cu and C powders were mechanical alloyed using various milling time (15, 30, 60, 90 and 120 min). After pressing (600 MPa) compacts were produced, the alloy powders were sintered for 1 h at 1150 °C in the atmosphere-controlled furnace. After sintering, the specimens were prepared for microstructure examinations and wear testing. Wear tests were done using pin-on-disc device under various loads (10–30 N), sliding distances (400–2000 m) and 1 ms⁻¹ constant sliding speed. Result of the study showed that powder size increased in Fe–Cu–C alloys up to 60 min mechanical alloying time. Maximum density and hardness values in Fe–Cu–C alloys were obtained in Fe–Cu–C alloy with 60 min mechanical alloying. In addition, the highest weight loss in wear tests was achieved in 120 min MA'ed specimen, while the lowest weight loss was achieved in 60 min MA'ed one.

Keywords Fe–Cu–C alloy · Powder metallurgy · Mechanical alloying · Microstructure · Wear

1 Introduction

Production of iron alloys by Powder Metallurgy (PM) method has become very popular and preferred more than other production methods [1, 2]. Using this method, high-quality parts with complex forms can be produced economically. It also makes easy to produce parts and components with different chemical composition in their final forms which do not require further machining [3, 4]. Some of the parameters important for determining the mechanical properties of the produced parts are: density/porosity in parts produced by this method, sintering temperature and duration, properties of the powders, alloying elements, etc. [5].

The most commonly used alloys in iron-based alloys produced by PM method are Fe–Cu–C alloys [6]. Pulleys,

sprockets, the camshaft, oil pump and valves, such as some used in the automotive industry in particular parts made from these alloy. [4, 7]. The production of these alloys by the PM method, a liquid phase sintering mechanism is generally preferred. In liquid phase sintering, a liquid phase must be obtained at the sintering temperature [7]. Copper (1083 °C), which has the lowest melting temperature in Fe–Cu–C alloys, causes liquid phase sintering as it becomes liquid at the sintering temperature. As liquid copper fills the pores within the part during sintering, the relative density of the produced parts increases which also improves the wear resistance owing to the hardness of the alloy produced. The highest dissolution of copper in the austenite (γ) phase is 8%–10% of the weight of iron. The dissolution of copper in iron (at room temperature) is 0.4% of the weight of ferrite (α) phase [8]. Addition of carbon to the alloy improves mechanical properties by reducing the expansion of copper by increasing the dihedral angle [8]. Fe–Cu–C alloy parts need to have good mechanical properties and high wear resistance in-service conditions as the parts operate under friction [9]. In addition, production conditions, production method, and chemical composition are factors that determine the microstructure of the alloy (especially grain size) and its mechanical properties [5, 10].

✉ Dursun Özyürek
dozyurek@karabuk.edu.tr

¹ Graduate School of Natural and Applied Sciences, Karabuk University, 78050 Karabuk, Turkey

² TOBB Technical Sciences Vocational School, Department of Machinery and Metal Technology, Karabuk University, 78050 Karabuk, Turkey

³ Department of Manufacturing Engineering, Technology Faculty, Karabuk University, 78050 Karabuk, Turkey

In a study Baroura et al. [11] investigated the effect of Cu amount (0.40, 0.55, 0.70, 0.85, 1) on Fe–Cu alloys produced by PM. They reported that as the amount of Cu increases, the hardness and density increase, and the best results are seen in alloys containing 1 wt% Cu. Salman et al. [12] examined the wear properties of Fe–Cu and Fe–Cu–C alloys produced by PM. They stated that with the C additive, the wear resistance of Fe–Cu–C alloys is better than Fe–Cu alloys. When the studies in the literature are examined, there are many studies on the effect of Cu and C amount in Fe–Cu–C alloys [2, 13–15]. Whereas, one of the determinant factors on the mechanical properties of alloys produced by PM method is particle size. The most important parameter in determining the powder size is the ball-powder ratio and milling time [16]. In studies conducted, the effect of milling time has not been investigated. Therefore, in this study the wear performances of Fe–Cu–C alloys, mechanically alloyed for various times were investigated and the effect of MA time on powder size, microstructure and wear behavior were examined.

2 Materials and Methods

In the experimental study, iron (99.7%, $d < 149 \mu\text{m}$, Aldrich), copper (99%, -325 mesh, $\%10$ max $+325$ mesh, Alfa Aesar) and carbon (99.5%, $d < 44 \mu\text{m}$, Aldrich) powders were used in the production of alloys. The chemical composition of Fe–Cu–C alloy used is given in Table 1.

The powders prepared were mechanically alloyed at 400 rpm in 5 various times (15–120 min) a planetary type alloying device (Fritsch Pulverisette). 1% ethanol was used as a process control chemical in order to prevent agglomeration and 10:1 ball/powder ratio in stainless steel milling cell with 250 ml capacity. To prevent powder from heating during the process, the device was stopped for 15 min after every 15 min of milling. Malvern brand laser particle sizer has been used for size measurements of alloyed powders. Alloyed Fe–Cu–C powders were cold-pressed (600 MPa) and compacts of $\text{Ø}12 \times 6$ mm were produced. The compacts were sintered for 1 h at $1150 \text{ }^\circ\text{C}$ in an atmosphere-controlled (10% hydrogen + nitrogen) environment and cooled in the furnace. After sintering, specimens were prepared with standard metallographic processes and then etched for 2–3 s in 2% Nital. The prepared specimens were investigated with Scanning Electron Microscopy (SEM + EDS), X-Ray Diffraction (XRD), hardness and density measurements. The Carl Zeiss Ultra Plus Gemini (FEG) brand was used in microstructure studies. X-ray diffraction (XRD) investigations were conducted in Rigaku D-Max Rint-2200 series brand device using copper (Cu) $K\alpha$

Table 1 In experimental study used of Fe–Cu–C alloy of chemical composition

Element	C	Cu	Fe
wt%	1	5	Balance

radiation. Hardness measurements were made as Vickers (HV2) in a Shimadzu brand micro hardness device by averaging 5 measurements obtained from every specimen. According to the Archimedes' principle density measurements were made in the Precisa XB200 h density measurement kit. Sample surfaces were polished with 1200-grit grinder paper before the wear tests and then polished with $6 \mu\text{m}$ diamond paste to obtain same surface quality in each sample. Wear tests were conducted under three various loads (10–30 N), five various distances (400–2000 m) and 1 ms^{-1} constant sliding speed on the pin-on-disc type device (ASTM:G99-5). AISI 4140 steel disc of a diameter of $\text{Ø}230$ mm, thickness of 20 mm and hardness of 60–64 HRC was used as counter material in wear tests. The disc was polished well ($R_a \sim 0.5 \mu\text{m}$) prior to conducting the wear tests. Weight losses were determined by weighing the worn samples on precision scales ($1/10,000$ g). The sample surfaces were cleaned with acetone before and after the wear test. Wear rates were calculated using the Eq. 1. After the wear tests were completed, the worn surfaces were examined with SEM.

$$W_a = \Delta G / (d \cdot P \cdot S) \quad (1)$$

where W_a is the wear rate (mm^3/Nm), ΔG is the weight loss (g), d is density (g/cm^3), P is the load weight (N), and S is the sliding distance (m).

3 Results and Discussion

3.1 Microstructure Examinations

Powder size variations of Fe–Cu–C alloys MA'ed at various times are given in Fig. 1.

Powder size variations of Fe–Cu–C alloys in Fig. 1 show that the powder size increases up to 60 min alloying time and

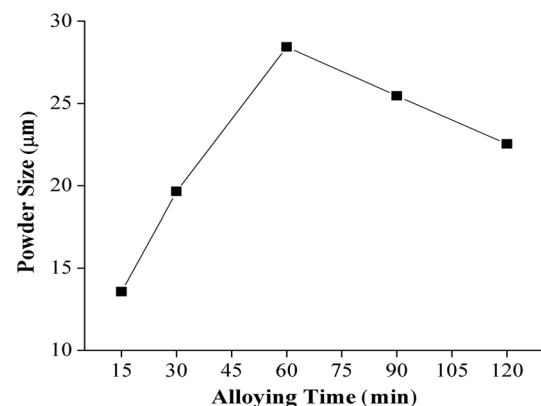


Fig. 1 Powder size variations of Fe–Cu–C alloys MA'ed at various times

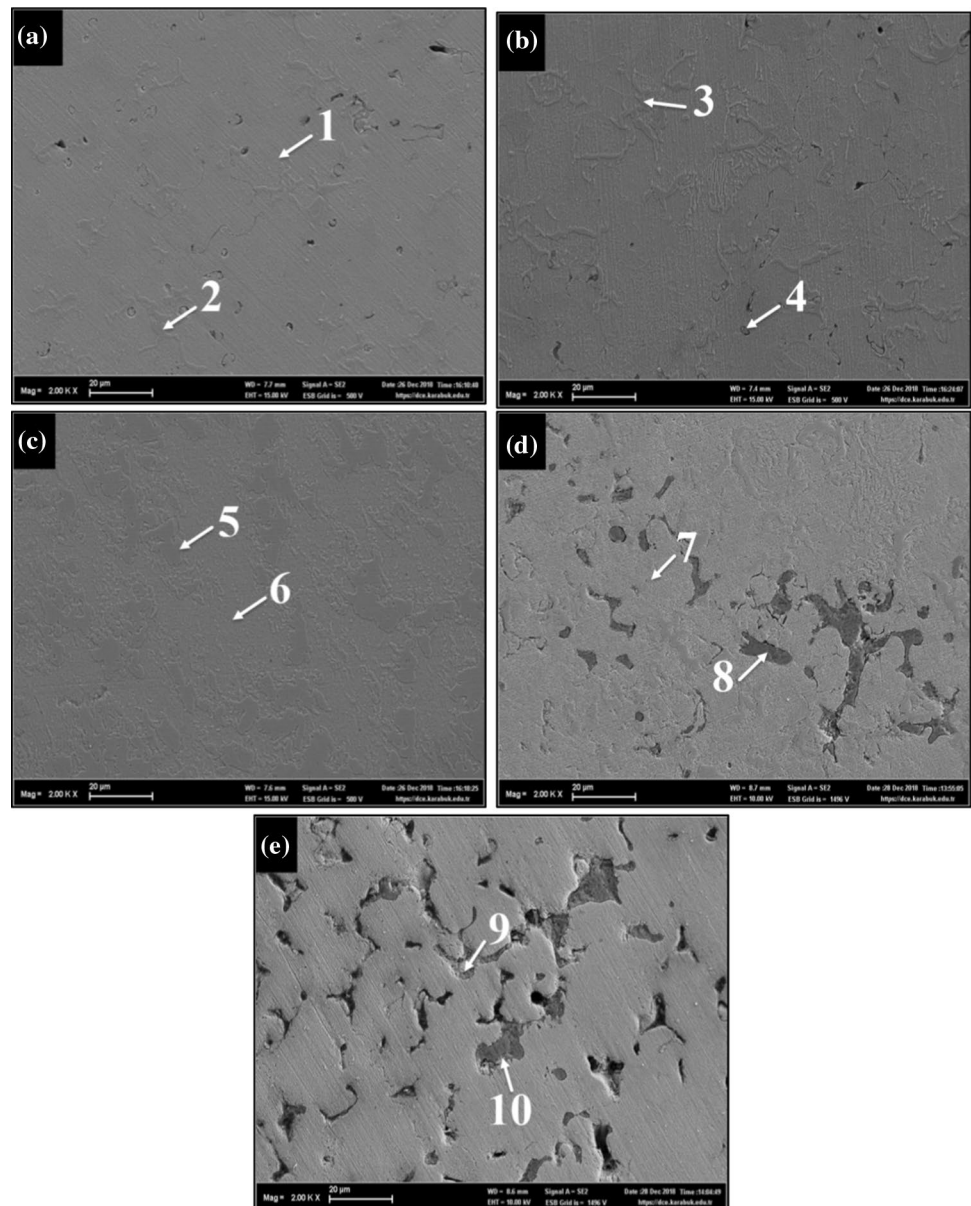
decreases in 90 and 120 min MA'ed powders. The MA process takes place in three stages: cold welding, deformation hardening and fracture [17]. During the process, cold welding takes place in the early stages of alloying by the continuous collision of powders between the balls and milling container walls. Therefore, powder size increases because of the cold welding. In the following stages, deformation hardening occurs in the particles grown by cold welding and powders are broken into smaller pieces which decrease the powder size [18]. Microstructure SEM images of MA'ed Fe–Cu–C alloys for various times are given in Fig. 2 and EDS (point) results obtained from the images are given in Table 2.

Microstructure SEM images in Fig. 2 show that as MA time increases, Cu is uniformly distributed within the matrix and concentrated in grain boundaries. Micro pores

Table 2 EDS analysis results of MA'ed Fe–Cu–C alloys at various times

Alloy	Location	C	Fe	Cu
15 min	1	9.23	87.05	3.72
	2	4.31	85.43	10.25
30 min	3	7.70	88.65	3.65
	4	2.73	81.73	15.54
60 min	5	8.89	87.17	3.94
	6	3.87	90.56	5.57
90 min	7	3.12	83.54	13.34
	8	7.93	88.55	3.52
120 min	9	6.52	83.13	10.34
	10	15.28	82.97	1.75

Fig. 2 Microstructure SEM images of MA'ed Fe–Cu–C alloys at various times **a** 15 min, **b** 30 min, **c** 60 min, **d** 90 min and **e** 120 min



are observed in the structure of the alloy MA'ed for 15 min. Micro pores decrease the structure up to 60 min of MA time. As the MA time increases (90 and 120 min), the pores formed in the structure become more apparent. The pores formed in the structure are concentrated in grain boundaries which can be explained by the reduction in formability due to deformation hardening and increased surface roughness of powders as a result of the continuous deformation between milling cell wall and ball during alloying of powders [18]. Annamalai et al. [19] stated that during sintering, liquid copper is concentrated along grain boundaries and then iron is dissolved in the lattice structure. EDS results also show that the dark regions (zone shown with 8 and 10) seen in the structures of 90 and 120 min MA'ed alloys are the iron phase. Due to the agglomeration of iron powders during MA, it is observed that they are localized in the dark region seen in the structure. SEM images in Fig. 2 also show that Cu and C rich regions exist in the structure up to 60 min alloying time. With increased alloying time, C rich regions are seen in the form of sediment in the structure. This is understood from the EDS point analysis results given in Table 2. As understood from the EDS analysis, Cu amount decreased in 60 min MA'ed alloys (zone shown with 5 and 6). This decrease is due to the grain coarsening seen as a result of cold welding occurring during mechanical alloying. With the alloying effect of Cu, which is softer than iron, it was completely embedded among Fe powders and remained homogeneous in the microstructure. XRD analysis results of MA'ed Fe–Cu–C alloys at various times are given in Fig. 3.

XRD analysis results in Fig. 3 show that α -Fe and γ phases are formed within the structure of 60 min MA'ed alloy. γ phase seen in the 60 min MA'ed alloy was not seen in other alloying times. Also, the formed α -Fe phase is more pronounced. Morakotjinda et al. [13] reported that both

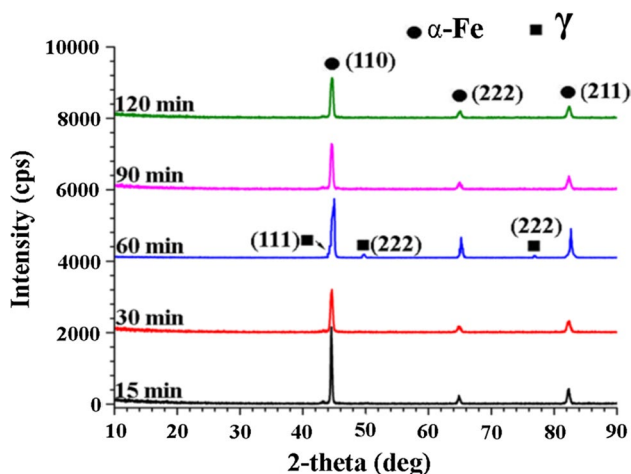


Fig. 3 XRD analysis results of MA'ed Fe–Cu–C alloys at various times

ferrite and austenite phases were formed at similar angles and peaks in Fe–6Cu–5C alloys produced by PM. The hardness and density variations of MA'ed Fe–Cu–C alloys in various times are given in Fig. 4.

Density variations in Fig. 4 show that the maximum density was 7.67 g/cm^3 in Fe–Cu–C alloy MA'ed for 60 min. As MA time increases, the density tends to decrease again. The density of the Fe–Cu–C alloy MA'ed for 120 min was measured as 6.65 g/cm^3 . This is also supported by the SEM images given in Fig. 2. Increasing closed pore ratio, caused by increased MA time, decreases the density. One of the reasons for closed pore formation is the powder surface roughness which increases with the MA time. While the surface roughness of the powders increases, actual measured density decreases as the milling time increases. Two effective methods are used in order to prevent partial density increase in formed powders. The first is the use of lubricants to allow particles slip over each other easily during formation, and the second is increasing the pressing load applied [18]. Yavuzer et al. [16] reported that the powder size of MA'ed AISI 304 stainless steel alloys decreased with increased alloying time. They stated that the decrease in density is caused by decreasing formability due to increased alloying time and deformation hardening occurred in powders. Figure 4 also shows that the hardness increases with increasing MA time and maximum hardness is obtained for the sample MA'ed for 60 min (217.9 HV). The hardness of the alloy tends to decrease with further increase in MA time. Hardness of the sample MA'ed for 120 min was measured as 172 HV. This decrease in hardness is associated with the amount of pore formed in the structure. In addition, the microstructure SEM images given in Fig. 2 support this situation. This result is consistent with a previous study [19]. The Cu atoms that dissolve in Fe increase lattice tension and prevent/limit

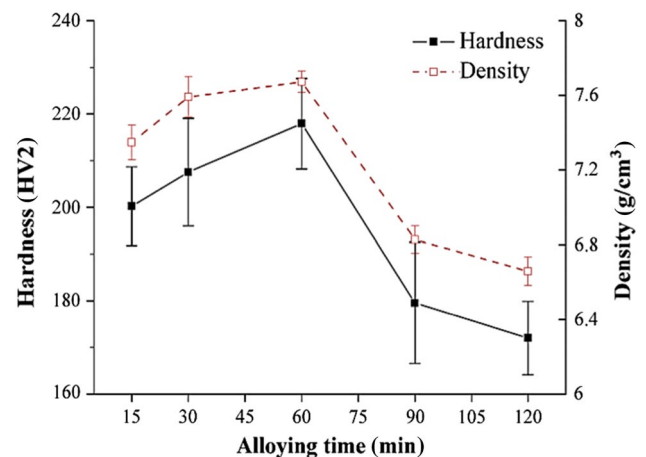


Fig. 4 Density and hardness variations of MA'ed Fe–Cu–C alloys at various times

dislocation movement. Prevention of the dislocation movement increases the strength of the material.

3.2 Wear Test Results

Variations in weight losses and wear rates under different loads (10, 20 and 30 N) of MA'ed Fe–Cu–C alloys at various times are given in Fig. 5.

The weight loss results in Fig. 5 show that the weight loss increases with the load. Similarly, the weight loss of alloys increases with increasing sliding distance. The highest weight loss under all loads (10, 20 and 30 N) used in the wear tests was achieved in alloy MA'ed for 120 min, while the lowest weight loss was achieved for 60 min. The results obtained are consistent with the hardness results given in Fig. 4. The hardness of alloy is an important parameter to determine its wear resistance. Similar results are reported by some other studies [10, 20]. Similarly, wear rate charts support weight loss results. The highest wear rate was achieved in alloy MA'ed for 120 min under 30 N load. In general, wear rates tend to decrease under all loads. This is due to the oxide layer constituted on the surface by the help of increased sliding distance, load and friction [21]. Wear ratio

results obtained under 30 N load shows that the wear ratios of samples MA'ed for 30, 90 and 120 min increase after 1200 m sliding distance. Micro-cracks occur just below the sample surface Due to plastic deformation that occurs during wear. As the sliding distance increases, micro-cracks progress and end in fractures. Wear particles moving away from the tribological system lead to increased wear rates. However, the increased surface roughness of the sample leads to an increased friction coefficient. The friction coefficient results given in Fig. 6.c support this situation. The friction coefficient variations of MA'ed Fe–Cu–C alloys under different loads are given in Fig. 6.

The friction coefficient of MA'ed Fe–Cu–C alloys given in Fig. 6 show that the friction coefficient is irregular. The friction coefficient for the alloys MA'ed for 15 and 30 min under 10 N load increased by the increasing sliding distance. Hard micro shavings produced by pin/disc dry friction can cause this increase in the friction coefficient. Wear particles break off the surface during the wear sink back into the surface and increase the surface roughness and the friction coefficient [22]. However, for the other MA times, the friction coefficients of the samples decrease by increasing sliding distance. Similar results are obtained under 20 N load. In

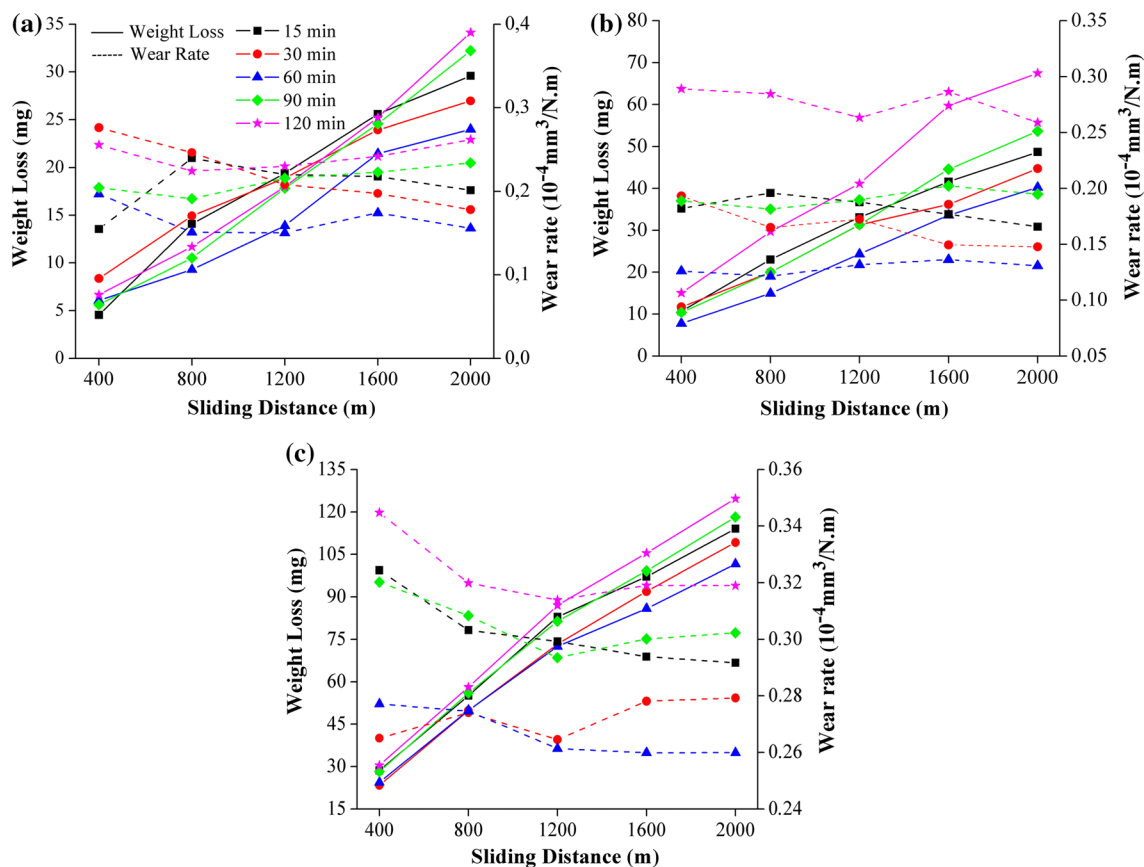


Fig. 5 Weight losses and wear rates of Fe–Cu–C alloys MA'ed at various times under different loads a 10 N, b 20 N and c 30 N

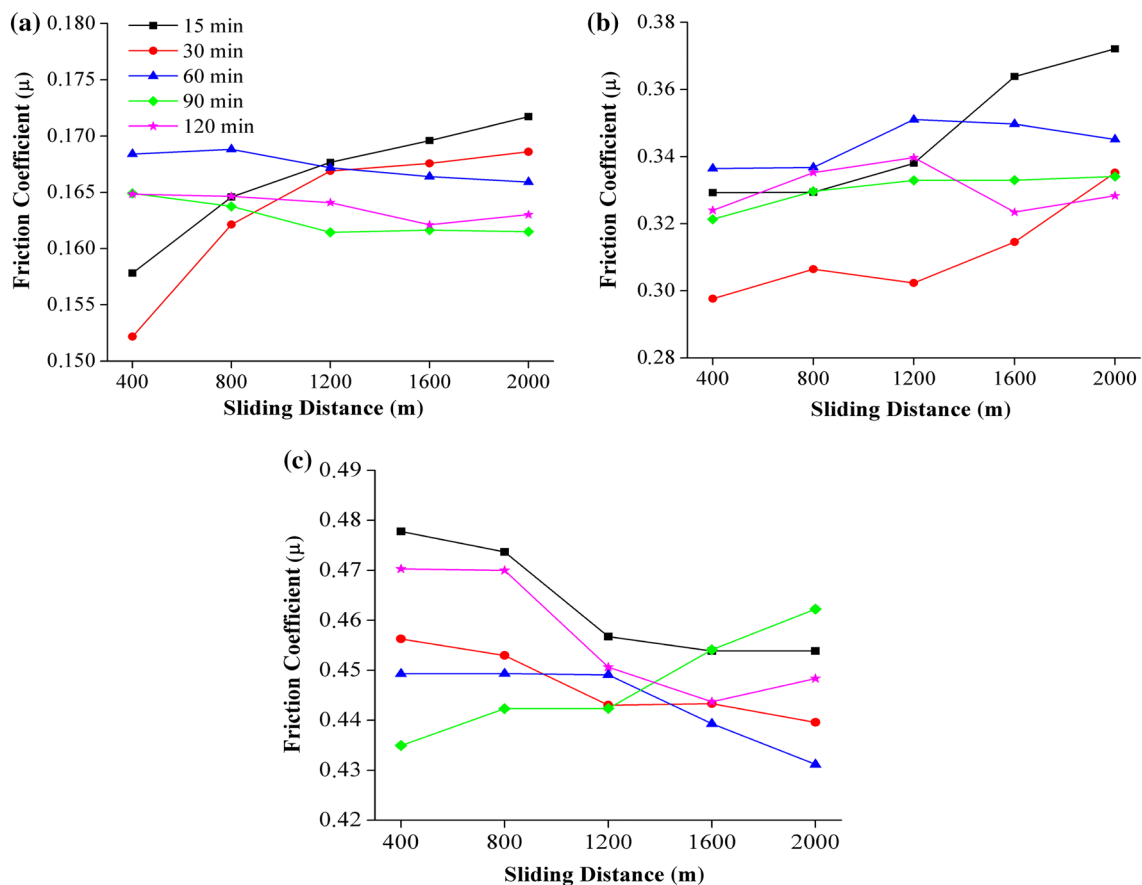


Fig. 6 Friction coefficient variations of Fe–Cu–C alloys MA'ed at various times under different loads **a** 10 N, **b** 20 N and **c** 30 N

the wear tests, the highest friction coefficient under both 10 and 20 N was obtained in alloy MA'ed for 60 min. The friction coefficient of alloys with high hardness is expected to be low. The results of the friction coefficient obtained in this study do not agree with this. The friction coefficient results under 30 N load shows that the friction coefficient decreases with increasing sliding distance. The lowest friction coefficient was achieved in Fe–Cu–C alloy having the highest hardness (MA'ed alloy for 60 min). Results obtained under load 30 N agree with this rule in general. As the applied load increases, the heat generated from friction increases. Oxides formed with increased heat (oxide layer formed due to thermal strain) act as a solid lubricant and decreased the friction coefficient. Chaurasia et al. [23] stated that this decrease in the friction coefficient is owing to the protective effect of iron oxide on the surface of the wear and that the weight loss also decreases with friction coefficient. Friction coefficient of the alloy MA'ed for 90 min increases beyond 1200 m sliding distance under 30 N load. This increase in friction coefficients is due to oxide particles sinking back into the surface. The worn surface SEM images of Fe–Cu–C alloys obtained under 30 N load are given in Fig. 7 and support this situation.

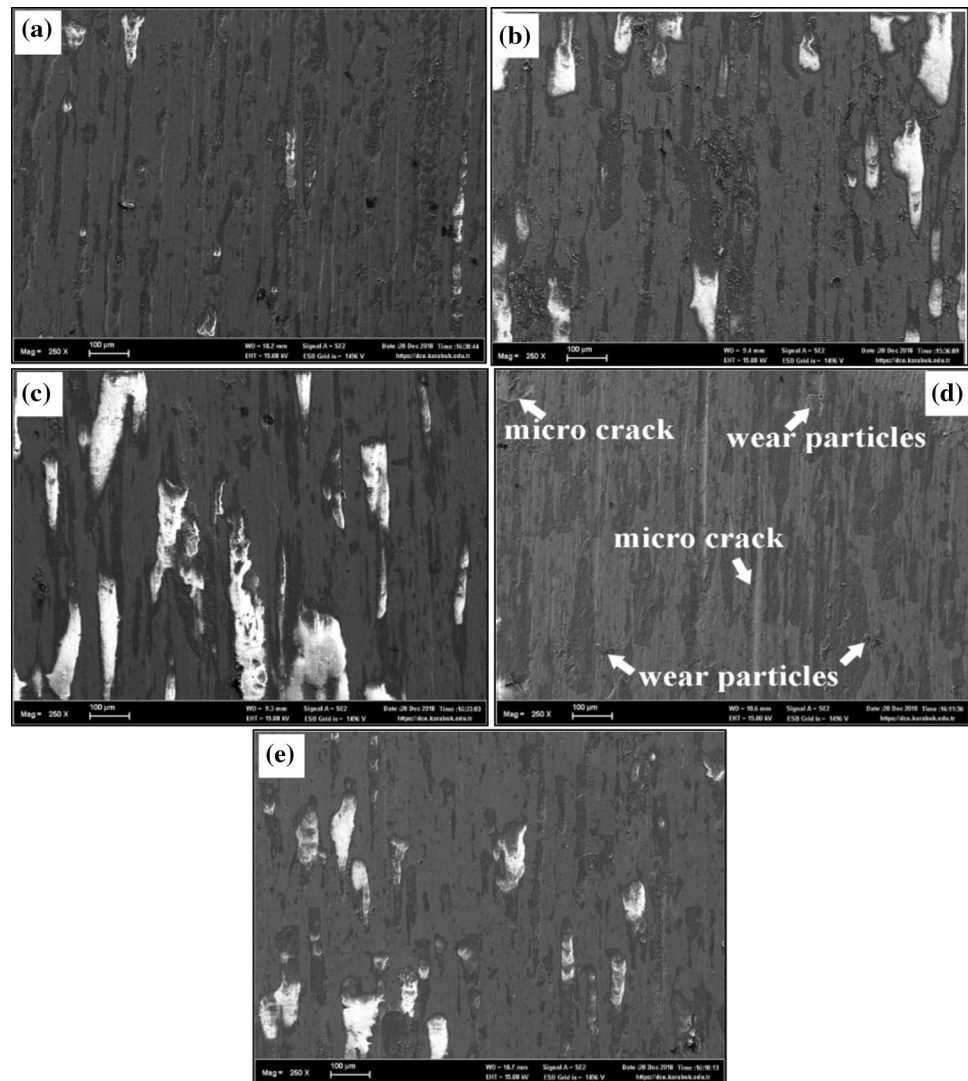
SEM images in Fig. 7, clearly show the deformation marks formed on the surface. It is understood that oxides (white regions) form on wear surfaces as the hardness increases. Wang and Danniger [21] obtained similar results. The oxide layer caused by the heat that is released as the load is increased during the wear test decreases the contact surface which also decreases wear rate, and the friction coefficient [24]. The wear ratio results (Fig. 5) and the friction coefficient results (Fig. 6) support this situation. However, micro-cracks in the worn surfaces and wear particles that sink back into the surface can also be seen. The resulting worn surface SEM images are in good agreement with the results of the friction coefficients results in Fig. 6c.

4 Conclusion

Below are some conclusions from the study on the effect of MA times on wear behavior of Fe–Cu–C alloy produced by PM method.

- Powder size analysis of MA'ed Fe–Cu–C alloys for various times shows an increase in powder size up to 60 min

Fig. 7 Worn surface SEM images of MA'ed Fe–Cu–C alloys at various times under 30 N load **a** 15 min, **b** 30 min, **c** 60 min, **d** 90 min and **e** 120 min



of alloying time. By the further increase of MA time, powder size tends to decrease.

- As the alloying time increased in MA'ed Fe–Cu–C alloys, Cu was observed to disperse homogeneously within the matrix and concentrate at grain boundaries.
- Maximum density and hardness values were obtained in Fe–Cu–C alloy MA'ed for 60 min.
- The highest weight loss under all loads (10, 20 and 30 N) used in wear tests was achieved in alloy MA'ed for 120 min and the lowest weight loss was obtained for the alloy MA'ed for 60 min.
- When all the results are evaluated, the highest hardness, density and wear resistance were obtained in 60 min MA'ed alloys.

Acknowledgements The authors are pleased to acknowledge the financial support for this study from Karabuk University Scientific Research Projects Department (KBÜ-BAP-17-YL-163).

References

1. N. Verma, S. Anand, J. Undergrad. Mat. Res. **2**, 53 (2006)
2. U. Cavdar, B.S. Unlu, E. Atik, Mater Tehnol. **48**, 977 (2014)
3. H.Ö. Gülsoy, M.K. Bilici, Y. Bozkurt, S. Salman, Mater. Des. **28**, 2255 (2007)
4. S.M. Sharma, A. Anand, Ind. Lubr. Tribol. **69**, 715 (2017)
5. S. Dhanasekaran, R. Gnanamoorthy, Mater. Des. **28**, 1135 (2007)
6. A. Zafari, P. Beiss, and C. Broeckmann, in *Proceedings Euro PM2010 world congress*, ss. pp 231–236 (2010)
7. K.S. Narasimhan, Mater. Chem. Phys. **67**, 56 (2001)
8. F. Nekatibeb, A.R. Annamalai, A. Upadhyaya, Trans. Indian Inst. Metals **64**(1–2), 81–84 (2011)
9. P. Sivakumar, N.G. Renganathan, P. Kumeravel, Int. J. Chem. Res. **5**, 2249 (2011)
10. S. Tekeli, A. Güral, Mater. Des. **28**, 1923 (2007)
11. L. Baroura, A. Boukhobza, A. Derardja, K. Fedouji, Int. J. Eng. Res. Afr. **34**, 5–12 (2018)
12. K.D. Salman, M.Z. Khalifa, A.M. Mohammd, J. Eng. Sustain. Dev. **20**, 64–74 (2016)
13. M. Morakotjinda, R. Krataitong, P. Wila, P. Siriphol, A. Daraphan, O. Coovattanachai, R. Tongsri, Chiang Mai. J. Sci. **35**, 258 (2008)

14. S.S. Rathore, V.V. Dabhade, *Trans. Indian Inst. Metals* **69**, 991–998 (2016)
15. X. Liu, Z.Y. Xiao, H.J. Guan, W. Zhang, F.L. Li, *Powder Metall.* **59**, 329–334 (2016)
16. B. Yavuzer, D. Özyürek, M. Gürü, *Acta Phys. Pol. A* **135**, 735 (2019)
17. C. Suryanarayana, *Prog. Mater. Sci.* **46**, 1 (2001)
18. I. Simsek, D. Ozyurek, *Powder Metall.* **60**, 384 (2017)
19. R. Annamalai, A. Upadhyaya, D. Agrawal, B. Mater. Sci. **36**, 447 (2013)
20. S. Tekeli, A. Güral, D. Özyürek, *Mater. Des.* **28**, 1685 (2007)
21. J.A. Wang, H. Danninger, *Wear* **222**, 49 (1998)
22. S. Mengistu, M.S. Bingley, M.S.A. Bradley, *P.I. Mech, Eng. EJ Pro* **218**, 221 (2004)
23. S.K. Chaurasia, U. Prakash, V. Dabhade, S.K. NathDry, *Mater. Today Proc.* **5**, 17170 (2018)
24. H. Chen, H.Y. Sun, *J. Adv. Mater. Res.* **415**, 707 (2012)

Publisher's Note Springer Nature remains neutral with regard to jurisdictional claims in published maps and institutional affiliations.